Separation and Purification Technology 194 (2018) 26–32

Contents lists available at ScienceDirect

Separation and Purification Technology

journal homepage: www.elsevier.com/locate/seppur

Electro-capture of heavy metal ions with carbon cloth integrated microfluidic devices

Francois-Marie Allioux[a,1,*], Pankaj Kapruwan[a,1], Nicholas Milne[b], Lingxue Kong[a], Jacques Fattaccioli[c], Yong Chen[c], Ludovic F. Dumée[a,*]

[a] Deakin University, Geelong, Institute for Frontier Materials, Waurn Ponds, VIC 3216, Australia
[b] Deakin University, Geelong, School of Engineering, Waurn Ponds, VIC 3216, Australia
[c] Ecole Normale Supérieure, Département de Chimie, ENS-CNRS-UPMC URM 8640, 75005 Paris, France

ARTICLE INFO

Keywords:
Electro-dialysis
Microfluidic
Ion-exchange membranes
Metal ion reduction
Resource recovery

ABSTRACT

A new multi-compartment microfluidic device was developed to simultaneously desalinate and recover valuable metal ions from aqueous streams mimicking metal plating and mining tailing wastewaters. Heavy and valuable metal ions including copper, zinc, nickel, silver and zinc/copper ionic mixtures were selectively transferred from the feed solution to a reduction chamber through ion-exchange membranes under the influence of an electrical field. A porous and conductive carbon cloth material was used as reduction platform, which led to improved desalination efficiencies, previously unachievable due to inevitable poisoning and degradation of the membranes at high current densities. The use of conductive carbon clothes enabled the recovery of the metal deposits, post reduction, through a simple electro-oxidation process. This novel microfluidic method, using ion-exchange materials as channel walls, has also the potential for the controlled decoration of materials with metal nanoparticle patterns and for the regeneration of rare earth trace contaminants by electro-sorption assisted electrodialysis.

1. Introduction

Globally, large amounts of industrial tailing effluents containing toxic and valuable metal ions and metal oxide particles are continuously generated by numerous industrial activities including mining, textile, tanning, electroplating and metal finishing operations [1,2]. Valuable metals such as copper, zinc, iron, nickel, silver and many more are often discarded and sent to landfill or waterbodies due to the lack of effective, onsite separation and recovery methods [2,3].

In addition to partial economic loss, the inadequate release of heavy metal ions poses serious environmental and health risks particularly prevalent in developing countries where insufficient water purification systems still remain in operation [4,5]. Traces of heavy metal elements can now be detected in the vegetal biomass due to the use of contaminated water and polluted soils [2]. However, stricter legislations and environmental awareness are now pushing for the implementation of waste minimization and management solutions [2,5]. Chemical precipitation, solvent extraction, membrane separation, electro-chemical reduction, ion-exchange separation and adsorption are among the main methods used for the remediation of heavy metal ions from diluted and concentrated solutions [2,3]. Each technique has specific advantages and limitations related to the durability, energy consumption and selectivity of the process [2,3]. Particularly, pressure-driven and electro-membrane separation processes such as electro-dialysis (ED), capacitive deionisation, nanofiltration, reverse osmosis and membrane distillation are proposed for the removal of heavy metal ions from liquid streams [6,7].

The advantages of membrane-based processes over traditional techniques include fewer chemical consumption, reduction of sludge volume, fast and limited materials regeneration as well as simpler and scalable module design [6]. Electro-separation and electro-membrane techniques used in electro-catalytic reactors offer additional advantages due to their ability to provide specific surfaces for the reduction or precipitation of the heavy metals in direct contact or through the membrane material [8,9]. ED is one of the most mature electro-membrane technologies widely used for the desalination of brackish water or for the pre-concentration of mineral salts [10,11]. During ED operation, ions and charged species are selectively separated from a feed to a concentrate solution across ion-exchange membranes (IEMs) under the influence of an electric potential gradient generated between two

* Corresponding authors.
E-mail addresses: f.allioux@research.deakin.edu.au (F.-M. Allioux), ludovic.dumee@deakin.edu.au (L.F. Dumée).
[1] These authors contributed equally to this work.

https://doi.org/10.1016/j.seppur.2017.10.064
Received 30 August 2017; Received in revised form 23 October 2017; Accepted 29 October 2017
Available online 31 October 2017
1383-5866/

electrodes. Many successful ED applications associated with a variety of IEM brands can be found in the literature for the removal and concentration of heavy metal ions in aqueous solutions such as zinc, copper and silver [12–15]. However, one of the key limitations of ED process applied for the desalination of heavy metal streams remains the poisoning of the IEMs due to the precipitation of the metal cations across the ion-exchange polymer matrix [16].

In this research, a novel, portable and scalable microfluidic ED process is demonstrated for the one-step concentration of heavy metal ions from model wastewaters and their reduction to solid metal onto a protective, porous and electrically conductive carbon cloth. The use of microfluidic devices allowed to study the electro-diffusion and electro-reduction of ionic species in a controlled and optimized process environment. Real mining, tanning, textile or electro-plating industrial waste effluents often include a variety of organic molecule pollutants such as dyes, pesticides or resins residues [17]. However, due to the selectivity of the IEMs towards dissociated and charged species, model solutions composed of copper, zinc, nickel and silver as well as zinc/copper ionic mixtures were prepared to study the recovery of the metal ions within the microfluidics system and mimic specifically electroplating and mining effluents. Hydrophobic macro-porous carbon cloths inserted between the cation-exchange membrane (CEM) and the anion-exchange membrane (AEM), which formed the surface of the microfluidic device, were used as reducing platforms. The experimental conditions were systematically varied to optimise the metal ions transfer rates and understand the deposition kinetics of metal ions across the carbon cloths. The metal deposits were then isolated using thermal or electrolytic methods. This novel approach where, for the first time, the microfluidics device is composed of ion exchange materials offered a quick and easy way for the recovery of heavy metals, which may be applied to a very large range of industrial feed sources from which ionic species may be recovered.

2. Materials and methods

2.1. Materials and chemicals

Sodium chloride (NaCl, AR grade, > 99.7% purity, M_w = 58.44 g·mol^{-1}) and sodium sulphate anhydrous (Na_2SO_4, analytical grade, > 99% purity, M_w = 142.04 g·mol^{-1}) were purchased from ChemSupply, SA, Australia. BioReagent grade copper sulphate pentahydrate ($CuSO_4{\cdot}5H_2O$, > 98% purity, M_w = 159.61 g·mol^{-1}), zinc sulphate heptahydrate ($ZnSO_4{\cdot}7H_2O$, > 99% purity M_w = 287.54 g·mol^{-1}), silver nitrate ($AgNO_3$, > 99%, M_w = 169.87 g·mol^{-1}), nickel sulphate heptahydrate ($NiSO_4{\cdot}7H_2O$, purum grade, > 95%, M_w = 280.86 g·mol^{-1}) and magnesium nitrate hexahydrate ($Mg(NO_3)_2{\cdot}6H_2O$, ACS reagent > 98%, M_w = 256.41 g·mol^{-1}) were sourced from Sigma-Aldrich, Castle Hill, NSW and used as received. The ionic solutions were prepared by dissolved a known quantity of salt crystals into deionized (DI) water under agitation.

The CEM and AEM, Selemion® (CMV and AMV brand names), were purchased from AGC Asahi Glass, Japan. Before starting the experiments, the membranes were first converted to Na^+ form for the cation-exchange type membranes and to Cl^- form for the anion-exchange type membranes using 0.5 M NaCl aqueous solutions. The membranes were immersed for 48 h under stirring in the NaCl solution, which was refreshed twice a day to ensure proper and complete exchange [18]. The properties of the Selemion® membranes are shown Table S2. A plain carbon cloth composed of woven carbon fibers was used as heavy metal ions collector. The plain carbon cloth (AvCarb 1071 HCB, 356 µm thickness) was ordered from FuelCellStore, TX, USA and used without any further modifications.

2.2. Characterization of materials and membranes

The morphology of the carbon cloths and membranes was studied by scanning electron microscopy (SEM) on a Jeol JSM 7800F. The elemental distributions on the surface of the carbon cloth samples were evaluated by Electron Dispersive X Ray Spectroscopy (EDS) analysis with an Oxford detector. SEM imaging was performed at 10 keV with a 10 mm working distance while elemental mapping was performed at 20 keV and with a 10 mm working distance.

The thicknesses of the IEMs and carbon cloths were measured using a digital micrometer (ProScitech, model SUM2-025). The average pore size distribution of the plain carbon cloths was measured using a capillary flow porometer (3–6 mbar pressure range, Porometer 3GZH Quantachrome Instruments, USA) after wetting the samples with Porofil® wetting solution (16.00 dyn·cm^{-1} surface tension).

The nature of the metal deposits on the carbon cloth was assessed by XRD measurements on a X'pert Pro (Panalytical, USA) equipped with a copper X-ray tube using Cu Kα radiation. The voltage and current were set to 40 kV and 30 mA during the experiments. Low background noise holders were used during the measurements.

The amount of deposited metal onto the carbon cloth was measured by weight difference of the carbon cloth before and after experiment on an AES 200-4C scale instrument with a precision of ± 0.2 mg. The carbon cloth was first dried in an oven at 80 °C for 30 min. The measurements were performed three times and the average values were reported. In addition, Thermogravimetric Analysis (TGA) tests were performed under air atmosphere using a Q50 TGA (TA instrument, USA) to assess the thermal stability of the samples and the amount of inorganic elements present across the carbon cloth. The experiments were performed with a fixed heating rate of 10 °C·min^{-1}, while the gas flow was maintained at 60 cm^3·min^{-1}.

Water contact angle measurements were performed with 4 µL DI water drops on the carbon cloth surface with a goniometer (KSV instruments model CAM 101). The tests were performed at three random locations on the surface of the sample. The images were acquired 5 s after the water drop impacted the membrane surface. The contact angles were calculated by fitting the image of the drops to the Young-Laplace equations and averaging with the obtained values on both sides of the drop using the optical tensiometer software, OneAttension Theta Lite.

2.3. Advanced electro-dialysis microfluidics set-up

Advanced ED tests were performed in a modified laboratory scale ED module fitted with microfluidics spacers set as a four-compartment stack made up of two AEMs and one CEM separated by spacers with specifically designed hydraulic pathways with effective transfer area of 4.60 cm^2 [19]. The width and depth of the channels across the spacers were 3.4 and 2 mm, respectively. Gold electrodes (40 × 40 mm^2) were used as cathode and anode materials to complete the ED stack. In a typical heavy metal recovery experiment, a carbon cloth piece (40 × 40 mm^2) was inserted between the pair of CEM and AEM facing the cathode in order to collect the heavy metal ions and protect the AEM from poisoning and degradation mechanisms (Fig. 1(a)). In addition, the desalination performance of the advanced ED process concept was compared to the desalination rates of metal ions by conventional ED process without carbon cloth present in the module. The experiments were carried out across a range of current densities (i) varying from 6.25 to 43.75 mA·cm^{-2} and performed at room temperature (20 °C). The flow rate across the spacers was set at 18 mL·min^{-1}, which represented a fluid flow velocity across the spacers of 4.3 cm·min^{-1}. Each test lasted for 30 min while a minimum of two sets of experiments were carried out in order to assess the reproducibility of the experiment.

The diluate compartment was fed with 250 mL of aqueous metal salt solutions. The concentrate and electrode compartments were fed with 250 and 500 mL of 0.1 M sodium sulphate aqueous solutions, respectively (Fig. 1(b)). The metal salt concentration in the feed solution was fixed at 0.1 M for copper and zinc sulphate salts and 0.05 M for nickel sulphate and silver nitrate. Magnesium nitrate was used as electrolyte

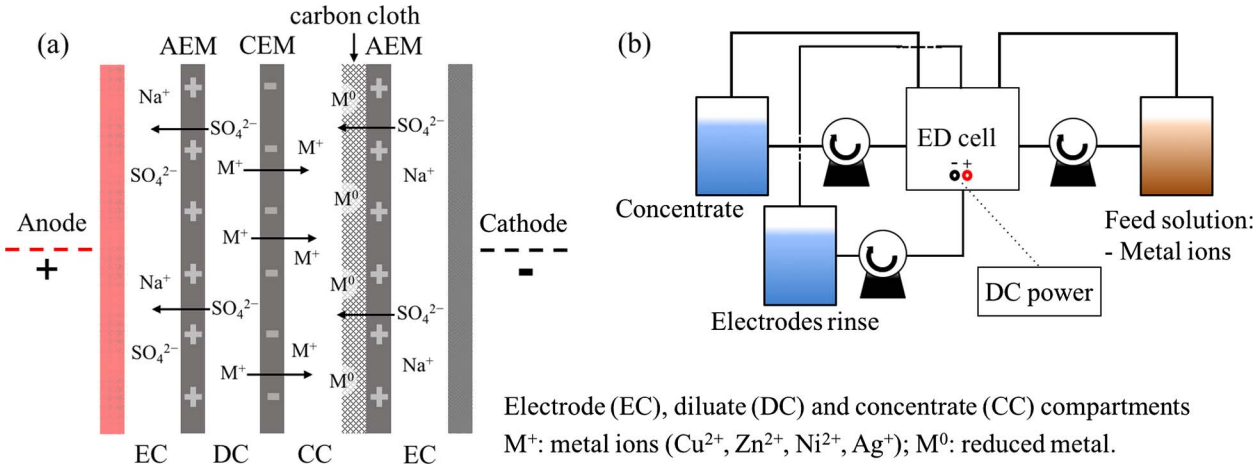

Fig. 1. Schematic of the novel microfluidic ED concept. (a) Design of the ED stack with the conductive carbon cloth element used for the reduction of heavy metal ions. (b) Schematic of the experimental set-up.

support for the experiments involving the recovery of silver from silver nitrate solutions in order to avoid the formation of insoluble silver complexes. The feed, concentrate and electrode streams were re-circulated across the ED stack with a 4 head peristaltic pump (John Morris, Scientific, USA). A DC power supply (BK Precision, 9124, LabVIEW software) was used to control and datalog the experimental current and voltage. The conductivity (χ) was recorded on a conductivity meter (CondTPS, WP-81) using the Termite Software (CompuPhase, USA).

2.4. Electro-desorption experiments

The electro-desorption experiments were performed in order to desorb the reduced metal deposits on the carbon cloths. An electrochemical cell constituted of two electrodes was used with a constant cell voltage of 1.5 V and 0.05 M of Na_2SO_4 as electrolyte support. A 316L grade stainless steel mesh (70 × 70 mesh size, 180 ± 10 µm thick, FuelCellStore, TX, USA) was used as the cathode material as the metal coated carbon cloth was used for the anode material. The metal coated carbon cloths were thoroughly rinsed with DI water and dried in an oven at 80 °C for 30 min before the start of the experiments.

3. Results and discussion

3.1. Carbon cloth properties

The properties and SEM image of the plain carbon cloth materials used as a collection template are shown in Supplementary Materials, Table S1 and Fig. S1(a), respectively. The carbon cloth presented a structure of plain woven carbon fibers with average pore size of 130 µm. The pore size distribution is shown in Fig. S1(b). The macroporous carbon cloth material provided a continuous medium for the electro-migration of ions and solvent molecules across the microfluidic module. The water contact angle measurement across the surface of the carbon cloth surface revealed a hydrophobic type material with a water contact angle value of 142 ± 5°. The hydrophobicity of the material was not considered to be an issue as the aqueous solutions were able to penetrate the woven carbon fiber structure due to the line pressure provided by the peristaltic pump and to the relatively low liquid entry pressure of the material. The water bubble point pressure of the material was measured at 0.0166 ± 0.0025 bar by capillary flow porometry demonstrating of a high permeation capability. Furthermore, the hydrophobicity of the carbon cloth could be an advantage for waste effluents containing large volume fraction of organic solvents such as toluene, relevant to the tanning industry [20].

3.2. Desalination and ionic transfer performance benchmarks

The desalination of sodium chloride (NaCl) solutions was first performed over a range of current densities in order to benchmark the desalination performance of the ED microfluidic device without the carbon cloth. The schematic representation of the microfluidic device and experimental set-up are presented Fig. 1(a–b), respectively. The fluxes of Na^+ across the CEM and removed from the diluate compartment are shown Fig. 2(a). The Na^+ fluxes increased linearly with the current density, which confirmed that the electro-migration of ions was not impaired by the module design or ion-exchange membrane materials. It was therefore assumed that the total current through the module without the carbon cloth inserted is carried by ions only and that the current leakage through the module and manifold system can be neglected [21]. In addition, the impact of the residence time of the solutions across the spacers on the ionic transport was investigated over a range of flow rates (Fig. S2). The Na^+ ionic fluxes were found to increase sharply from 12 mL·min^{-1} to 18 mL·min^{-1} before reaching a plateau for higher flow rates. The flow rate was therefore fixed at 18 mL·min^{-1} for the electro-diffusion experiments.

Similarly, the desalination of $CuSO_4$ solutions was performed without carbon cloth over a range of current densities to set a benchmark for the electro-diffusion and reduction experiments across the microfluidics cell (Fig. 2(b)). The fluxes of Cu^{2+} were found to be almost half that of the fluxes of Na^+ at the same current density value. Na^+ and Cu^{2+} have different size, valency and hydration shell, they will therefore migrate across the IEM materials at different rates. As an example, the hydrated ionic radius of Cu^{2+} (600 pm) is 25% larger than the hydrated ionic radius of Na^+ (450 pm) [22]. The lower transport rates of Cu^{2+} in the CEM material was due to the greater electrostatic interaction with the oppositively charged functional groups of the CEM [23]. However, the flux of Cu^{2+} did not further increase above 31.25 mA·cm^{-2} as the limiting current density was reached and a steady state situation was established between the electro-migration of Cu^{2+} across the CEM materials and the diffusive transport of Cu^{2+} in the bulk solution [24]. The experiments performed, above the limiting current density, at 43.75 mA·cm^{-2}, without carbon cloth resulted in scaling and strongly damaging the AEM facing the cathode as seen in Fig. S3. This effect is related to the concentration polarization of the metal ions where the depletion of ions at the surface of the AEM leads to an increased voltage drop. The electrical current is unable to flow due to the absence of ions, which induces water-splitting phenomena with extreme localized pH changes and thus precipitation of the multivalent ions as hydroxides [11,21].

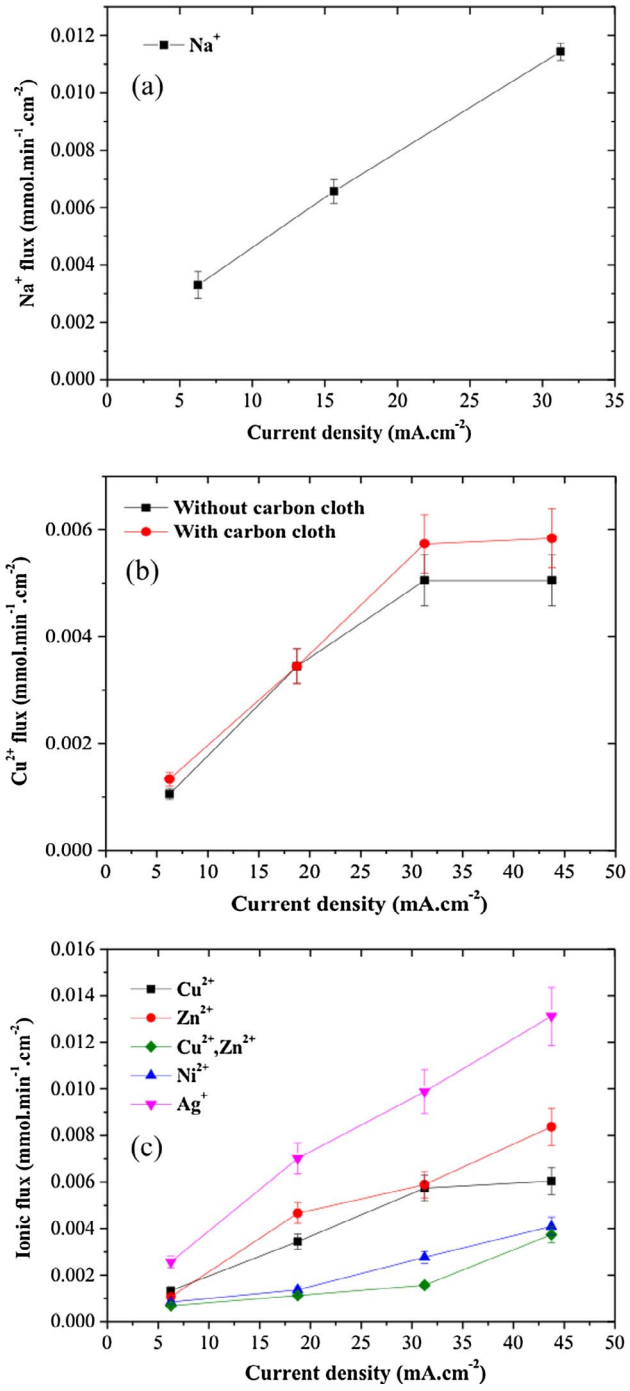

Fig. 2. Ionic fluxes across the ED microfluidic device from the diluate to the concentrate compartment as a function of the current density. (a) Sodium (Na^+) ionic fluxes without carbon cloth. (b) Copper (Cu^{2+}) ions fluxes with and without carbon cloth. (c) Ionic fluxes with carbon cloth for the different heavy metal ions studied.

3.3. Recovery of the metal ions

The recovery experiments were then performed using the ED module by inserting the carbon cloth material in the concentrate compartment, in contact with the AEM facing the cathode (Fig. 1). Fig. 2(b–c) shows the ionic fluxes in the ED module as a function of the current densities. The Cu^{2+} fluxes with carbon cloth were similar to the ones without carbon cloth (Fig. 2(b)), which indicated that the carbon cloth did not affect the electro-migration and diffusive transport within the ED module. The Cu^{2+} fluxes followed a similar linear increased with a maximum reached for a current density of 31.25 mA·cm^{-2}. However, the AEM material was not degraded at higher current density (43.75 mA·cm^{-2}). A possible explanation may be that the carbon cloth acted as an electron sink inhibiting the water splitting at the surface of the AEM. Similarly, the fluxes of Ni^{2+}, Zn^{2+}, Ag^+ and Cu^{2+}:Zn^{2+} stoichiometric mixture are shown in Fig. 2(c). Also, Ag^+ exhibited the greatest mobility across the CEM material with fluxes almost twice as high as the other heavy metal ions due to the lower valence and hydrated radius (250 pm) of the silver ion [25–27]. However, the fluxes of the Cu^{2+}:Zn^{2+} stoichiometric mixture were found to be lower than the fluxes for the single ionic species due to the competitive transport of both cations across the CEM material [26]. The CEM was shown to be permeable to monovalent and divalent heavy metal cations confirming the applicability of ED technology to the treatment of wastewaters contaminated with heavy metal ions.

The heavy metal ions transferred into the concentrate compartment were then captured on the carbon cloth material. Similarly to cathodic reduction processes, a range of reduction reactions can occur across the negatively charged carbon cloth, including water reduction and local alkalinity increase [28]. The SEM images of the carbon cloth scaled with the metal deposits over the range of current densities are shown in FigS. 3 and -4. The reduction of the heavy metal ions onto the carbon cloth started at the lowest current density (6.25 mA·cm^{-2}). As expected, the reduction of metal ions was found to be more important at the greatest current densities due to the increased availability of electrons across the carbon cloth. The copper and zinc species were reduced in clusters starting from the initial metal seeds present at the surface of the carbon fibers (Fig. 3). On the other hand, the nickel and silver depositions were found to be more scattered across the surface of the carbon fibers as seen in Fig. 4, which may be due to the seeding growth affinity of the metal ions and the carbon surface [29]. The SEM images presented a greater coverage of the carbon cloth by the metal deposits as a function of the current densities, which was directly correlated to the ion fluxes, as previously presented in Fig. 2.

The measured weight gains of the carbon cloths at the end of the experiments showed similar results as seen in Fig. 5(a). The deposition of the heavy metal ions was found to follow a linear increase as a function of the current densities. Silver deposition was the greatest with a 16% weight increase at 43.75 mA·cm^{-2}, indicating a direct correlation with both the ionic fluxes and the deposition rates (Fig. 2(c)). The weight increases due to the deposition of Cu^{2+}, Zn^{2+} and Ni^{2+} were similar ranging from 0.7 to 1.4 wt% at 6.25 mA·cm^{-2} and 7–9 wt% at 43.75 mA·cm^{-2}. However, the deposition of Cu^{2+}:Zn^{2+} stoichiometric mixture on the carbon cloth showed a superior weight increase as compared to the deposition of the single metal species. The nature of the deposits, in terms of composition and crystallinity, was then characterised using the EDX and XRD techniques.

The EDX elemental analysis of the carbon cloth coated with copper species (Fig. S4(a)) revealed that the clusters are composed almost exclusively of copper (46.86 at.%) with only 5.4 at.% of oxygen and the remaining comprised of carbon. The EDX elemental analysis of the mixed copper/zinc clusters (Fig. S4(b)) showed an interestingly greater ratio of zinc element (16.93 at.%) over copper (6.96 at.%). The electrochemical reduction of mixed metal ions in solution typically involves more complex reduction mechanisms than the reduction of single metal ions in solution [30,31]. One explanation for the greater ratio of zinc element over copper might involve a mixed mechanism of electro-reduction Cu^{2+} and sequential alkaline precipitation of zinc species with OH^- resulting from the water reduction [31]. The electro-reduction of Cu^{2+} occurred before Zn^{2+} due to the higher value of standard reduction potentials (E^0). The presence of sulphur (4.12 at.%), sodium (2.71 at.%) and high oxygen content (40.63 at.%) also supported the mixed electro-reduction and precipitation mechanism.

The EDX elemental analysis of the carbon cloth coated with nickel and silver species is shown in Fig. S4(c–d), respectively. The EDX elemental analysis revealed that a negligible amount of sulphur and magnesium counter-ions is still present across the carbon cloth,

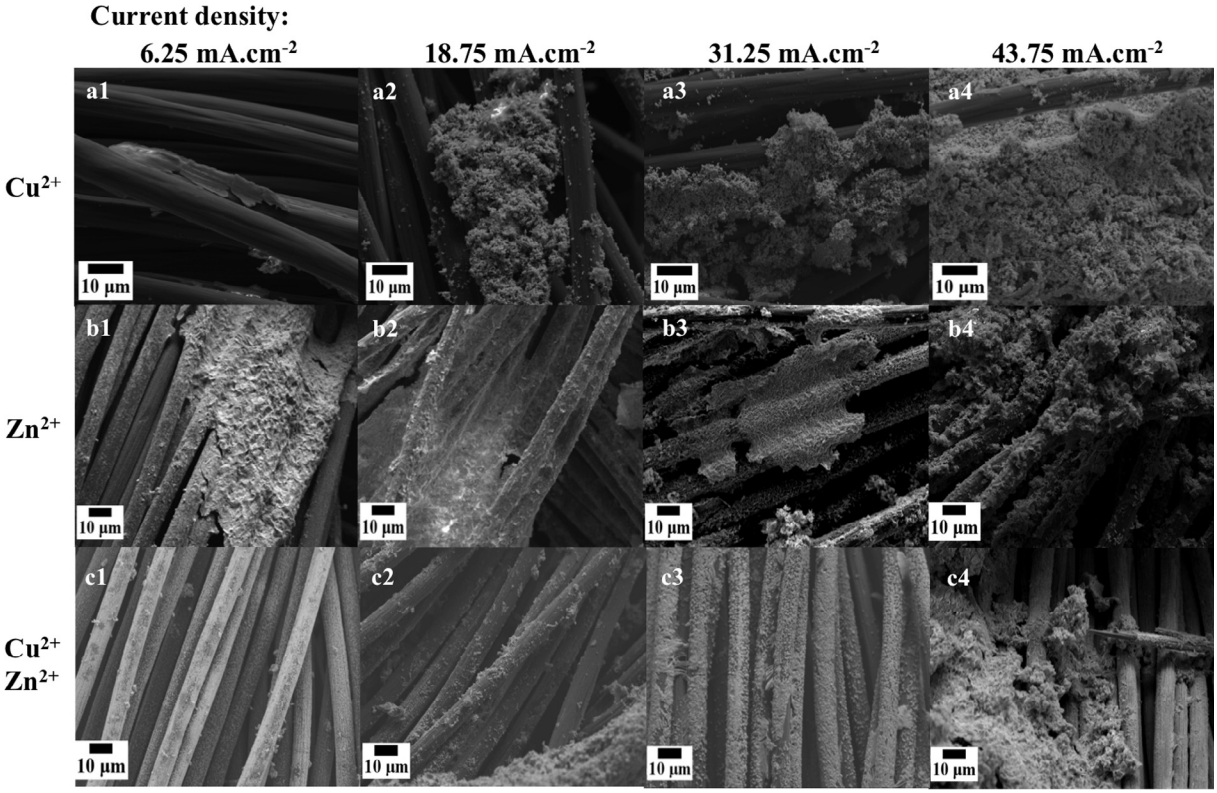

Fig. 3. SEM characterization of the metal deposits. (a) Copper, (b) zinc and (c) mixed copper/zinc deposits on the carbon cloth as a function of the current densities at 6.25 (1), 18.75 (2), 31.25 (3) and 43.75 (4) mA·cm^{-2}.

indicating that the precipitation of metal salts is less plausible. However, the oxygen content was found to be as high as 30.48 and 9.53 wt% for the nickel and silver coated carbon cloths, respectively. The formation of silver and nickel oxide could be explained by the local increase of pH across the carbon cloth due to the water reduction. In alkaline solutions both nickel and silver were found to form hydroxide compounds in competition to the electro-reduction process [14,32,33].

The crystalline nature of the metal deposits was analysed using XRD measurements. A low noise sample holder was used in order to reveal the crystalline structure of the samples without interferences (Fig. 5(b)). The spectrum (*a*) corresponding to the carbon cloth was characteristic of the carbon fiber type materials with a broad peak at 2θ = 25° [34]. The XRD spectrum of the carbon cloth with the silver deposition (*b*) showed a crystalline metallic phase with peaks at 2θ = 38 and 44.5°, corresponding to the diffractions of Ag(1 1 1) and Ag(2 0 0), respectively [35]. However, the presence of peaks at 2θ = 32.4 and 33.1° revealed the presence of silver oxides (Ag_2O) [36,37], which was in good agreement with the EDX elemental analysis results. The spectrum (*c*) corresponds to the nickel deposit onto the carbon cloth. The broad peak at 2θ = 44.6° may correspond to the combined crystalline split peak of metal Ni(1 1 1) and nickel oxide NiO(2 0 0) [38]. The spectra of the carbon cloth with the copper deposit (*d*) showed strong

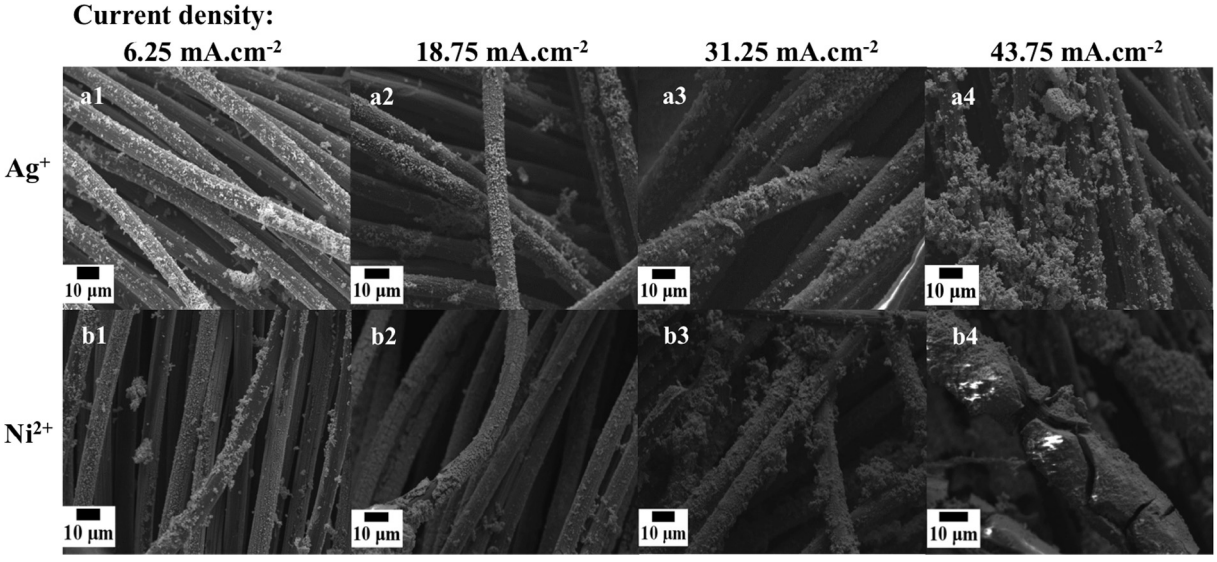

Fig. 4. SEM characterization of the metal deposits. (a) Silver and (b) nickel deposits on the carbon cloth as a function of the current densities at 6.25 (1), 18.75 (2), 31.25 (3) and 43.75 (4) mA·cm^{-2}.

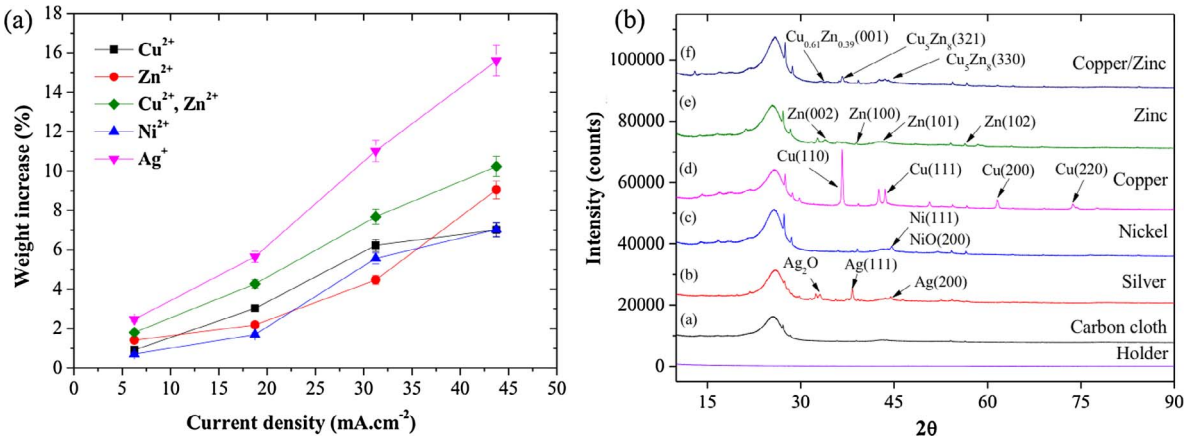

Fig. 5. Physical characterization of the metal deposits. (a) Weight variation of the carbon cloths after the deposition experiments as a function of the current densities. (b) XRD analysis of the pristine carbon cloth and the metal coated carbon cloths at 31.25 mA·cm^{-2} (spectra were offset by 15.000 units).

Cu(1 1 0), Cu(1 1 1), Cu(2 0 0) and Cu(2 2 0) metal peaks at 2θ = 36.68, 42.45, 50.68 and 73.74°, respectively [39,40]. The zinc coated carbon cloth showed only minor peaks (*e*) of Zn(0 0 2), Zn(1 0 0), Zn(1 0 1) and Zn(1 0 2) at 2θ = 34.15, 38.93, 42.56 and 54.23°, respectively [41,42]. Finally the XRD spectrum of the mixed copper/zinc deposit (*f*) revealed the deposition of a Cu-Zn alloy with a *β* phase *β*-$Cu_{0.61}Zn_{0.39}$(0 0 1) at 2θ = 33.40° and γ phases γ-Cu_5Zn_8(3 2 1) and γ-Cu_5Zn_8(3 3 0) at 2θ = 36.75 and 43.77°, respectively [43]. The combined XRD and EDX analysis of the mixed copper/zinc deposit therefore indicate the presence of both a reduced Cu-Zn alloy compound and a deposition of amorphous metal salt species across the carbon cloth.

3.4. Metal recovery and desorption experiments

Samples of the coated carbon cloth (2–3 mg) were collected from an area where the metal deposits were visible. The depositions of metal species were found to follow the hydraulic path created by the spacer. As a reminder the serpentine-shaped spacer used for these experiments also led to a serpentine-shaped deposition pattern across the surface of the carbon clothes as seen in Fig. S5(a-b). At high current density, 43.75 mA·cm^{-2}, the deposition rate was not consistent across the fluid pathway and extended outside the effective transfer area delimited by the spacers (Fig. S5(c)). This effect was attributed to the diffusion and reduction of cations across the woven carbon fiber structure. Therefore, the TGA experiments were considered to be qualitative only. The TGA analysis of the pristine and coated carbon cloths after the electro-deposition experiments are shown in Fig. S5(d–e). The pristine carbon cloth material was thermally stable up to 695 °C and 50–80 °C lower when coated with copper deposits due to the catalytic activity of the copper metal [44]. Similarly, the silver deposition promoted the thermal degradation of the carbon cloth by 50 °C, however, no significant effects on the thermal degradation of the carbon cloth were found for the nickel, zinc and copper/zinc deposits (Fig. S5(e)). Nevertheless, the recovery of metal could be performed via the thermal degradation of the carbon cloth substrate.

The electro-chemical desorption experiments were then performed within an electro-chemical cell using a full size carbon cloth with copper deposited at 31.25 mA·cm^{-2} and constituted the anode. The cathode was made of a conductive stainless steel mesh composed of woven stainless steel fibers (70 µm in diameter), which presented surface indentations oriented parallel to the fiber axis (Fig. 6(a–b)). The copper metal deposited on the carbon cloth was oxidized and subsequently reduced on the surface of the stainless steel cathode. Fig. 6(c–d) show the pattern deposition of the copper particles at the surface of a stainless steel fibers after 30 min of experiment. The surface EDX analysis of the stainless steel fibers revealed deposits of pure copper metal with a low oxygen content (3.8 wt%, Fig. S6). The sizes of the copper

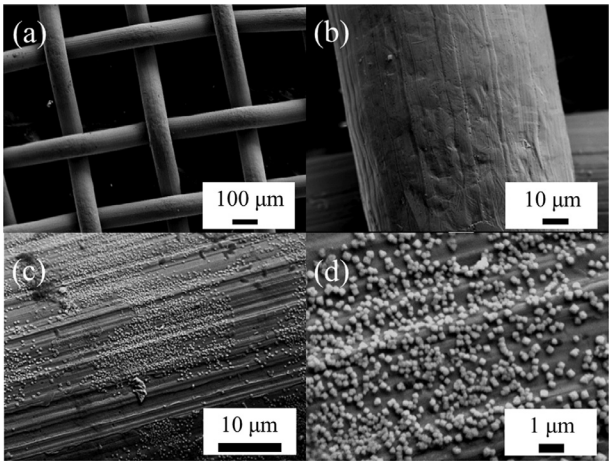

Fig. 6. SEM characterization of the stainless steel cathode. (a) and (b) Pristine stainless steel mesh. (c) and (d) Coated stainless steel mesh with copper deposits after the electro-desorption experiments.

crystals were between 50 and 300 nm with a square pyramidal crystallite structure probably resulting from the surface roughness of the fibers. In this experiment, the copper coated on the carbon cloth was successfully recovered on a stainless steel mesh cathode. In addition, no visible degradations of the carbon cloth materials were observed at the end of the electro-chemical desorption experiments indicating a reusability of the material and therefore limiting the material cost of the process.

4. Conclusions

The combined desalination and recovery of an aqueous stream containing valuable single and mixed heavy metal ions was performed in a novel ED microfluidics set-up. A carbon cloth element was inserted in the concentrate compartment and acted as an electron sink limiting the adverse consequences of the polarization concentration effect on the IEMs. The heavy metal ions were captured on the carbon cloth surface by a mixed mechanism of electro-chemical reduction and alkaline precipitation. The metal deposition rates were found to increase linearly with the current densities and ionic fluxes. The copper and zinc deposits were composed of pure electro-reduced metal as the silver and nickel deposition presented a mixed of metal and metal oxide species characteristic to electro-chemical reduction processes in alkaline conditions. The copper metal deposits reduced onto the carbon cloth were successfully re-oxidized and reduced on a stainless steel mesh highlighting the easy recovery of the metal deposits. The copper/zinc ionic

mixture was partially reduced as an alloy onto the carbon cloth, however, amorphous metal salt species were also detected. In order to treat streams composed of mixed heavy metal ions and further increase the selectivity of the desalination and reduction processes, the use of specific complexion agents should be investigated. In addition, the microfluidic ED process developed here could be easily scaled to a full industrial-size ED stack due the increasing availability of large woven carbon fiber materials and apply to the large scale processing and refining of mineral ore. Alternatively, an array of microfluidic ED devices arranged in parallel could be considered to scale up the recovery process. Although the method presented here focused on the removal and recovery of valuable heavy metal ions, the coated carbon clothes could also be valorised as final by-products with potential applicability. Indeed, the carbon cloth coated with silver crystals could be valued as anti-bacterial filters or as catalytic electrodes when coated with copper and nickel species.

Acknowledgements

F.-M. Allioux would like to thank the Institute for Frontier Materials, Deakin University, Victoria, Australia for funding his PhD scholarship and AINSE Ltd for providing financial assistance (PGRA Award - 30290). L.F. DUMEE acknowledges Deakin University for his Alfred Deakin Post-doctoral Fellowship.

Funding

This research did not receive any specific grant from funding agencies in the public, commercial, or not-for-profit sectors.

Appendix A. Supplementary material

Supplementary data associated with this article can be found, in the online version, at http://dx.doi.org/10.1016/j.seppur.2017.10.064.

References

[1] M.C. Jung, Heavy Metal Concentrations in Soils and Factors Affecting Metal Uptake by Plants in the Vicinity of a Korean Cu-W Mine, Sensors (Basel, Switzerland) 8 (2008) 2413–2423.
[2] R.A. Wuana, F.E. Okieimen, Heavy metals in contaminated soils: a review of sources, chemistry, risks and best available strategies for remediation, Isrn Ecol. 2011 (2011).
[3] F. Fu, Q. Wang, Removal of heavy metal ions from wastewaters: a review, J. Environ. Manage. 92 (2011) 407–418.
[4] O.B. Olafisoye, T. Adefioye, O.A. Osibote, Heavy metals contamination of water, soil, and plants around an electronic waste dumpsite, Pol. j. Environ. Stud 22 (2013) 1431–1439.
[5] P.B. Tchounwou, C.G. Yedjou, A.K. Patlolla, D.J. Sutton, Heavy metal toxicity and the environment, Molecular, clinical and environmental toxicology, Springer, 2012, pp. 133–164.
[6] X. Wei, X. Kong, S. Wang, H. Xiang, J. Wang, J. Chen, Removal of heavy metals from electroplating wastewater by thin-film composite nanofiltration hollow-fiber membranes, Ind. Eng. Chem. Res. 52 (2013) 17583–17590.
[7] J. Lv, K.Y. Wang, T.-S. Chung, Investigation of amphoteric polybenzimidazole (PBI) nanofiltration hollow fiber membrane for both cation and anions removal, J. Membr. Sci. 310 (2008) 557–566.
[8] C. Zhou, D. Chin, Copper recovery and cyanide destruction with a plating barrel cathode and a packed-bed anode, Plat. Surf. Finish. 80 (1993) 69–78.
[9] S. Caprarescu, D. Vaireanu, A. Cojocaru, I. Maior, V. Purcar, A 3-cell electrodialysis system for the removal of copper ions from electroplating wastewater, Optoelectron. Adv. Mater., Rapid Commun. 5 (2011) 1346–1351.
[10] T. Xu, C. Huang, Electrodialysis-based separation technologies: a critical review, AIChE J. 54 (2008) 3147–3159.
[11] H. Strathmann, Electrodialysis, a mature technology with a multitude of new applications, Desalination 264 (2010) 268–288.
[12] G. Wisniewska, T. Winnicki, Electrodialytic desalination of effluents from zinc-coating processes: removal of Zn2+ and CL− ions from model solutions, Desalination 84 (1991) 163–176.
[13] Ü.B. Öğütveren, S. Koparal, E. Özel, Electrodialysis for the removal of copper ions from wastewater, J. Environ. Sci. Health, Part AEnviron. Sci. Eng. 32 (1997) 749–761.
[14] A. Güvenç, B. Karabacakolu, Use of electrodialysis to remove silver ions frommodel solutions and wastewater, Desalination 172 (2005) 7–17.
[15] K.H. Choi, T.Y. Jeoung, Removal of zinc ions in wastewater by electrodialysis, Korean J. Chem. Eng. 19 (2002) 107–113.
[16] T. Xu, Ion exchange membranes: state of their development and perspective, J. Membr. Sci. 263 (2005) 1–29.
[17] O. Lefebvre, R. Moletta, Treatment of organic pollution in industrial saline wastewater: a literature review, Water Res. 40 (2006) 3671–3682.
[18] Y. Tanaka, Ion Exchange Membranes: Fundamentals and Applications, Elsevier, 2015.
[19] F.-M. Allioux, L. He, F. She, P.D. Hodgson, L. Kong, L.F. Dumée, Investigation of hybrid ion-exchange membranes reinforced with non-woven metal meshes for electro-dialysis applications, Sep. Purif. Technol. 147 (2015) 353–363.
[20] G. Lofrano, S. Meriç, G.E. Zengin, D. Orhon, Chemical and biological treatment technologies for leather tannery chemicals and wastewaters: a review, Sci. Total Environ. 461 (2013) 265–281.
[21] H.-J. Lee, H. Strathmann, S.-H. Moon, Determination of the limiting current density in electrodialysis desalination as an empirical function of linear velocity, Desalination 190 (2006) 43–50.
[22] C.D. Hodgman, Handbook of Chemistry and Physics, LWW1951.
[23] A. Chapotot, G. Pourcelly, C. Gavach, Transport competition between monovalent and divalent cations through cation-exchange membranes. Exchange isotherms and kinetic concepts, J. Membr. Sci. 96 (1994) 167–181.
[24] H. Strathmann, Ion-exchange Membrane Separation Processes, Elsevier, 2004.
[25] A.F. Wells, Structural Inorganic Chemistry, Oxford University Press, 2012.
[26] A.T. Cherif, A. Elmidaoui, C. Gavach, Separation of Ag+, Zn2+ and Cu2+ ions by electrodialysis with monovalent cation specific membrane and EDTA, J. Membr. Sci. 76 (1993) 39–49.
[27] J. Kielland, Individual activity coefficients of ions in aqueous solutions, parameters 4 (1937) 4.5.
[28] J. Paul Chen, L.L. Lim, Recovery of precious metals by an electrochemical deposition method, Chemosphere 60 (2005) 1384–1392.
[29] A.D. Pomogailo, G.I. Dzhardimalieva, Nanostructured materials preparation via condensation ways, Springer, 2014.
[30] L. Doulakas, K. Novy, S. Stucki, C. Comninellis, Recovery of Cu, Pb, Cd and Zn from synthetic mixture by selective electrodeposition in chloride solution, Electrochim. Acta 46 (2000) 349–356.
[31] M.D. Machado, E.V. Soares, H.M. Soares, Selective recovery of copper, nickel and zinc from ashes produced from Saccharomyces cerevisiae contaminated biomass used in the treatment of real electroplating effluents, J. Hazard. Mater. 184 (2010) 357–363.
[32] C. Natarajan, H. Matsumoto, G. Nogami, Improvement in electrochromic stability of electrodeposited nickel hydroxide thin film, J. Electrochem. Soc. 144 (1997) 121–126.
[33] Y. Wan, X. Wang, S. Liu, Y. Li, H. Sun, Q. Wang, Effect of electrochemical factors on formation and reduction of silver oxides, Int. J. Electrochem. Sci 8 (2013) 12837–12850.
[34] H. Long, T. Shi, H. Hu, S. Jiang, S. Xi, Z. Tang, Growth of Hierarchal Mesoporous NiO Nanosheets on Carbon Cloth as Binder-free Anodes for High-performance Flexible Lithium-ion Batteries, Sci. Rep. 4 (2014) 7413.
[35] W. Ye, C. Shen, J. Tian, C. Wang, C. Hui, H. Gao, Controllable growth of silver nanostructures by a simple replacement reaction and their SERS studies, Solid State Sci. 11 (2009) 1088–1093.
[36] N.L. Yong, A. Ahmad, A.W. Mohammad, Synthesis and characterization of silver oxide nanoparticles by a novel method, Int. J. Sci. Eng. Res. 4 (2013) 155–158.
[37] B.M. Jović, V.D. Jović, Electrochemical formation and characterization of Ag2O, J. Serb. Chem. Soc. 69 (2004) 153–166.
[38] J.T. Richardson, R. Scates, M.V. Twigg, X-ray diffraction study of nickel oxide reduction by hydrogen, Appl. Catal., A 246 (2003) 137–150.
[39] H. Shen, F. Wang, Y. Ding, J. Yang, Electrodeposition process for the fabrication of copper dendrites film with stable superhydrophobicity, Acta Metall. Sin. (Engl. Lett.) 26 (2013) 641–646.
[40] L. Chen, Y. Zhang, P. Zhu, F. Zhou, W. Zeng, D.D. Lu, R. Sun, C. Wong, Copper salts mediated morphological transformation of Cu2O from cubes to hierarchical flower-like or microspheres and their supercapacitors performances, Sci. Rep. 5 (2015) 9672.
[41] N. Alias, A.A. Mohamad, Morphology study of electrodeposited zinc from zinc sulfate solutions as anode for zinc-air and zinc-carbon batteries, J. King Saud Univ Eng. Sci. 27 (2015) 43–48.
[42] P.S. da Silva, E.P.S. Schmitz, A. Spinelli, J.R. Garcia, Electrodeposition of Zn and Zn–Mn alloy coatings from an electrolytic bath prepared by recovery of exhausted zinc–carbon batteries, J. Power Sources 210 (2012) 116–121.
[43] F.L.G. Silva, D.C.B. do Lago, E. D'Elia, L.F. Senna, Electrodeposition of Cu–Zn alloy coatings from citrate baths containing benzotriazole and cysteine as additives, J. Appl. Electrochem. 40 (2010) 2013–2022.
[44] S.J. Chiu, W.H. Cheng, Thermal degradation and catalytic cracking of poly(ethylene terephthalate), Polym. Degrad. Stab. 63 (1999) 407–412.